Terrestrial Planet Finder Interferometer (TPF-I)

Response to Astro2010 Request for Information for Proposed Activities

P. R. Lawson[†] (Jet Propulsion Laboratory, California Institute of Technology)

O. Absil (Univ. Liège)
R. L. Akeson (Caltech)
J. Bally (Univ. Colorado)
R. K. Barry (NASA GSFC)
C. A. Beichman (Caltech/JPL)
A. J. Booth (JPL)
P. Bordé (IAS)
J. Breckinridge (JPL)
D. Cole (JPL)
V. Coudé du Foresto (Obs. Paris)
W. C. Danchi (NASA GSFC)
R. Danner (NGAS)
D. Defrère (Univ. Liège)
C. Eiroa (U. Autónoma Madrid)
P. Falkowski (Rutgers Univ.)
R. O. Gappinger (JPL)
C. Hanot (Univ. Liège)
T. Henning (MPIA)
T. Herbst (MPIA)
P. M. Hinz (Univ. Arizona)
S. Hunyadi (JPL)
D. C. Hyland (Texas A&M)
K. J. Johnston (USNO)
L. Kaltenegger (CfA)
J. F. Kasting (Penn State Univ.)
A. Ksendzov (JPL)
L. Labadie (MPIA)
B. F. Lane (Draper Laboratory)
O. P. Lay (JPL)
A. Léger (IAS)
R. Liseau (Univ. Stockholm)
B. Lopez (Obs. Cote d'Azur)
F. Malbet (Obs. Grenoble)
S. R. Martin (JPL)
D. Mawet (JPL & Univ. Liège)
B. Mennesson (JPL)
R. Millan-Gabet (Caltech)
M. C. Noecker (Ball Aerospace)
J. Nishikawa (NAOJ)
M. Pesenson (Caltech)
R. D. Peters (JPL)
A. C. Quillen (Univ. Rochester)
S. Ragland (WMKO)
S. Ridgway (NOAO)
S. Rinehart (NASA GSFC)
H. Röttgering (Univ. Leiden)
D. P. Scharf (JPL)
S. Seager (MIT)
E. Serabyn (JPL)
W. A. Traub (JPL)
S. C. Unwin (JPL)
D. J. Wilner (Harvard CfA)
N. J. Woolf (Univ. Arizona)
M. Zhao (Univ. Michigan)

31 March 2009

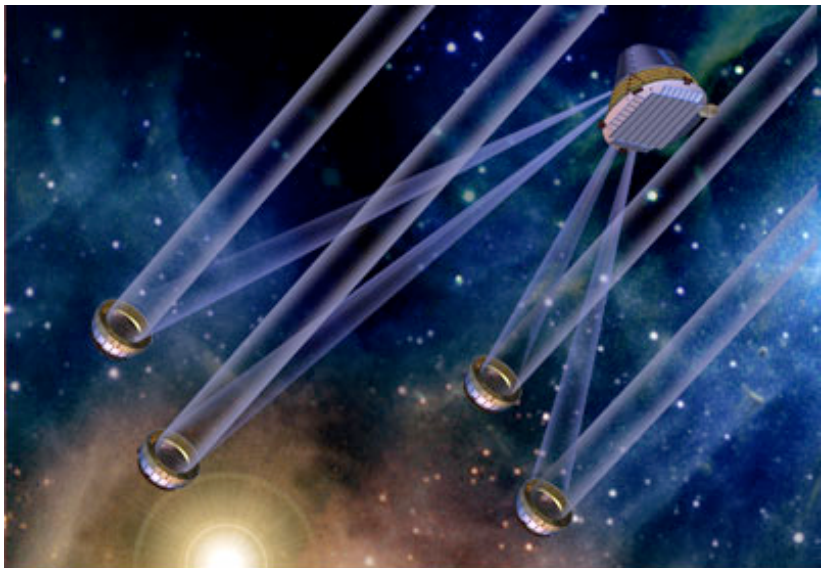

http://planetquest.jpl.nasa.gov/TPF-I/tpf-I_index.cfm

[†]Corresponding author: Peter R. Lawson. Tel: (818) 354-0747
Jet Propulsion Laboratory, Pasadena, CA 91109. Email: Peter.R.Lawson@jpl.nasa.gov

EXECUTIVE SUMMARY

Understanding the origins of life on Earth and finding evidence of life elsewhere in the Universe are two of the major goals of science. Where did we come from? Are we alone? Key advances in technology in the next decade would enable the Terrestrial Planet Finder Interferometer (TPF-I), a mission with the high-angular resolution and high dynamic range sensitivity necessary to find evidence of life around a statistically significant number of stars.

The Terrestrial Planet Finder was proposed to the 2000 Decadal Survey as an array of four 3.5-m telescopes in a free-flying nulling interferometer array, diffraction limited at 2 μm, operating at < 50 K, and with observations over the 6–18 micron wavelength band. Its science goals were to survey ~150 stars to determine the frequency of planetary systems with planets the size of Earth or larger in orbits where liquid water might be expected to be stable. It would perform low-resolution spectroscopy on ~50 planetary systems, looking for CO_2, H_2O, and on about 5 targets search for O_3 or CH_4. Half of the mission time was to be devoted to general astrophysics, with the observation of ~1000 infrared targets.

Over the past decade, TPF-I has been developed in parallel with the European Darwin mission. By 2007, a common TPF/Darwin mission architecture was defined in which the aperture size of the telescopes was reduced to 2.0 m, the complexity of the collector spacecrafts was greatly simplified, and the sky coverage was increased to 99% as measured over the course of a year. This architecture is the baseline design described in this pages. Table 1 illustrates the properties of this point design, described in more detail later in the text.

TPF-I is a flagship class mission. It would be launched on a large launch vehicle (such as a Delta-IV Heavy) with telescopes and combiner packaged in a cylindrical stack. A cruise stage would take the observatory to a Sun-Earth L2 Halo orbit for a mission duration of 5 years, with a 10 year goal.

TPF-I has benefited from directed funding from NASA for its technology development, as recommended by the 2000 Decadal Review. Parallel work has also been undertaken at the European Space Agency. Technology development for TPF-I has been extremely successful:

1. Mid-infrared single-mode fibers have been demonstrated in chalcogenide glass and silver-halide material to provide the required spatial filtering for nulling interferometry.
2. Nulling experiments have demonstrated the flight requirement of 1×10^{-5} nulling, using a 34% bandwidth centered at a wavelength of 10 μm.
3. The requisite levels of performance of formation-flying guidance, navigation and control algorithms have been demonstrated in the lab, both in simulation and using robotic testbeds. Although demonstrations have yet to been undertaken in space demonstrating TPF-I requirements, these results suggest that the challenges of formation flying are well understood and tractable.
4. The cryocooler work first initiated by TPF-I has been highly successful; adaptations of TPF-I cryocooler technology are now being used for the MIRI instrument on JWST.

Having a fundamentally sound architecture of the mission, and a clear understanding of the technology requirements, we requests an investment of $300M in the 2010–2020 decade to validate nulling technology in a cryogenic vacuum environment, and to enable formation flying demonstrations in space within the context of an international collaboration. This would bring nulling technology to TRL 6, formation flying technology to TRL 9, and enable a relatively short Phase A of the mission beginning around 2020.

1. KEY SCIENCE GOALS

The major scientific objectives of TPF-I are: (1) search for and detect any Earth-like planets in the habitable zone around nearby stars; (2) characterize Earth-like planets and their atmospheres, assess habitability, and search for signatures of life; (3) carry out a study of gas giants and icy planets, as well as terrestrial planets within the 5 AU of nearby stars (at a nominal distance of 10–15 parsecs from the Sun); (4) carry out a program of comparative planetology; and (5) enable a program of revolutionary general astrophysics. A mission lifetime of 5 years, possibly extended to 10 years, is foreseen.

TPF-I would be designed to detect terrestrial exoplanets around nearby stars and measure their spectra (e.g., Beichman et al. 1999; Cockell et al. 2009). These spectra would be analyzed to establish the presence and composition of the planets' atmospheres, to investigate their capability to sustain life as we know it (habitability), and to search for signs of life. TPF-I would also have the capacity to investigate the physical properties and composition of a broader diversity of planets, to understand the formation of planets, and to search for the presence of potential biosignature compounds. The range of characteristics of planets is likely to exceed our

Table 1. Illustrative Properties of a TPF-I Observatory Concept

Parameter	4-Telescope Chopped X-Array Emma Design
Collectors	Four 2-m diameter spherical mirrors, diffraction limited at 2 μm operating at 50 K
Array shape	6:1 rectangular array
Array size	400 × 67 m to 120 × 20 m
Wavelength range	6–18 μm
Inner working angle	13–43 mas (at 10 μm , scaling inversely with array size)
Angular resolution	2.4 mas to 8.2 mas (at 10 μm, scaling inversely with array size)
Field-of-view	1 arcsec at 10 μm (FWHM)
Null depth	10^{-5}at 10 μm (not including stellar size leakage)
Spectral resolution Δλ/λ	25 (for planets); 100 for general astrophysics
Sensitivity	0.3 μJy at 12 μm in 14 hours (5σ)
Target Stars	153 (F, G, K, and M main-sequence stars)
Detectable Earths	72 (within 2 years of mission time, assuming 1 Earth per star)
Exozodiacal emission	Less than 10 times our solar system
Biomarkers	CO_2, O_3 , H_2O, CH_4
Field of regard	Instantaneous 45° to 85° from anti-Sun direction, 99.6% of full sky over one year.
Orbit	Sun Earth L2 Halo orbit
Mission duration	Design life of 5 years with a 10 year life goal
Launch vehicle	Heavy-class launch vehicle, such as Delta IV H-19
Launch Mass	8200 kg total: 1770 kg combiner; 1190 kg reflector × 4; 1670 kg cruise stage
Required Power	4570 Watts combiner; 720 Watts reflector; 550 Watts cruise stage
Pointing: Combiner	60 arcsec control, 30 arcsec knowledge (3σ)
Pointing: Reflector	1.7 arcsec control, 0.3 arcsec knowledge, 0.8 arcsec stability (3σ)

experience with the planets and satellites in our own Solar System.

Biomarkers are detectable species whose presence at significant abundance requires a biological origin (Des Marais et al. 2002). They are the chemical ingredients necessary for biosynthesis (e.g., oxygen [O_2] and CH_4) or are products of biosynthesis (e.g., complex organic molecules, but also O_2 and CH_4). Our search for signs of life is based on the assumption that extraterrestrial life shares fundamental characteristics with life on Earth, in that it requires liquid water as a solvent and has a carbon-based chemistry. Therefore, we assume that extraterrestrial life is similar to life on Earth in its use of the same input and output gases, that it exists out of thermodynamic equilibrium, and that it has analogs to bacteria, plants, and animals on Earth (Lovelock 1975).

Candidate biomarkers that might be detected by TPF-I with a low-resolution instrument include O_2, O_3, and CH_4. There are good biogeochemical and thermodynamic reasons for believing that these gases should be ubiquitous byproducts of carbon-based biochemistry, even if the details of alien biochemistry are significantly different than the biochemistry on Earth. Production of O_2 by photosynthesis allows terrestrial plants and photosynthetic bacteria (cyanobacteria) to use abundant H_2O as the electron donor to reduce CO_2, instead of having to rely on scarce supplies of hydrogen (H_2) and hydrogen sulfide (H_2S). Oxygen and nitrous oxide (N_2O) are two very promising bio-indicators. Oxygen is a chemically reactive gas. Reduced gases and oxygen have to be produced concurrently to produce quantities large enough to be detectable in disk-averaged spectra of terrestrial planet atmospheres, as they react rapidly with each other. N_2O is a biomarker in the Earth's atmosphere, being produced in abundance by life but only in trace amounts by natural processes. Although a relatively weak feature in the Earth's spectrum, it may be more pronounced in terrestrial exoplanet atmospheres of different composition or host-star spectral type. Currently, efforts are ongoing to explore the plausible range of habitable planets and to improve our understanding of the detectable ways in which life modifies a planet on a global scale.

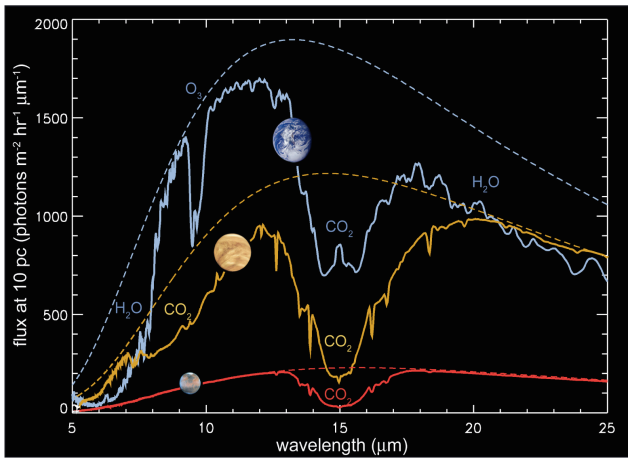

Figure 1. Spectra of Earth, Venus, and Mars, showing their blackbody curves and the presence of water vapor, ozone, and carbon dioxide. (F. Selsis, ENS Lyon)

In the mid-IR, the classical signature of biological activity is the combined detection of the 9.6-µm O_3 band, the 15-µm CO_2 band, and the 6.3-µm H_2O band or its rotational band that extends from 12 µm out into the microwave region (Selsis & Despois 2002). The oxygen and ozone absorption features in the visible and thermal infrared, respectively, could indicate the presence of photosynthetic biological activity on Earth any time during the past 50% of the age of the Solar System. In the Earth's atmosphere, the 9.6-µm O_3 band is a poor quantitative indicator of the O_2 amount, but an excellent qualitative indicator for the existence of even traces of O_2. The O_3 9.6-µm band is a very nonlinear indicator of O_2 for two reasons. First, for the present atmosphere, low-resolution spectra of this band show little change with the O_3 abundance because it is strongly saturated. Second, the apparent depth of this band remains nearly constant as O_2 increases from 0.01 times the present atmosphere level (PAL) of O_2 to 1 PAL (Segura et al.

2003). The primary reason for this is that the 15 micron O_3 absorption band is generated only in the upper (cool) side of the CO_2-induced stratospheric temperature inversion, so that increased CO_2 simply increases the heating at the inversion and pushes the cool side higher, to a region where there are fewer CO_2 molecules per unit volume, thus keeping the absorption feature approximately constant in strength, independent of the overall CO_2 mixing ratio.

Methane is not readily identified using low-resolution spectroscopy for present-day Earth, but the CH_4 feature at 7.66 μm in the IR is easily detectable at higher abundances (Kaltenegger et al. 2007). When observed together with molecular oxygen, abundant CH_4 can indicate biological processes (see also Lovelock 1975; Segura et al. 2003). Depending on the degree of oxidation of a planet's crust and upper mantle, non-biological mechanisms can also produce large amounts of CH_4 under certain circumstances.

With a low-resolution spectrum covering the 6–18 μm region, TPF-I would be able to determine directly the effective temperature of the planet. Coupled with the total flux density and orbital location, TPF-I measurements also determine a planet's radius and albedo. In the mid-IR, the most studied and robust signature of biological activity is the combined detection of the 9.6-μm O_3 band, the 15-μm CO_2 band, and the 6.3-μm H_2O band or its rotational band that extends longward from 12 μm (Selsis et al. 2002; DesMarais et al. 2002). Other spectral features of potential biological interest include methane, ammonia, nitrous oxide and nitrogen dioxide, which would not be detectable by TPF-I in an exact Earth analog, but might be present in measurable quantities in a potentially habitable (or inhabited) planet at earlier evolutionary phase. When a reduced species like methane is detected along with O_3 we would have a very strong indication of a biological release (Lovelock 1980; Sagan et al. 1993). The three strongest bands in the Earth-analog spectrum, O_3 band, CO_2 band, and H_2O (see Figure 1, courtesy of F. Selsis and G. Tinetti), could all be detected with a spectral resolution of 10–25.

Types of Stars: We expect that Earth-like planets are most likely to be found around stars that are roughly similar to the Sun. Therefore, target stars will include main sequence F, G, and K stars. However, M stars may also harbor habitable planets, and the nearest of these could be investigated. TPF-I, with its adjustable long baseline, has an advantage over the TPF-C coronagraph in that TPF-I can select an angular resolution suitable to observing planets orbiting M stars where the habitable zone is located very close to the surface of the star.

Terrestrial Planets: Considering the radii and albedos or effective temperatures of Solar System planets, the mission must be able to detect terrestrial planets, down to a minimum terrestrial planet defined as having 1/2 Earth surface area and Earth albedo. In the infrared, the minimum detectable planet would be one with an infrared emission corresponding to the surface area and optical albedo, positioned in the orbital phase space stipulated below.

Habitable Zone: TPF-I should search the most likely range as well as the complete range of temperatures within which life may be possible on a terrestrial-type planet. In the Solar System, the most likely zone is near the present Earth, and the full zone is the range between Venus and Mars. The habitable zone (HZ) is here defined as the range of semi-major axes from 0.7 to 1.5 AU scaled by the square root of stellar luminosity (Kasting et al. 1993; Forget & Pierrehumbert 1997). The minimum terrestrial planet must be detectable at the outer edge of the HZ.

Orbital Phase Space: The distribution of orbital elements of terrestrial type planets is presently unknown, but observations suggest that giant-planet orbits are distributed roughly equally in semi-major axis, and in eccentricity up to those of the Solar System planets and larger. Therefore, TPF-I must be designed to search for planets drawn from uniform probability distributions in semi-major axis over the range 0.7 to 1.5 AU and in eccentricity over the range 0

to 0.35, with the orbit pole uniformly distributed over the celestial sphere with random orbit phase.

Giant planets: The occurrence and properties of giant planets may determine the environments of terrestrial planets. The field of view and sensitivity must be sufficient to detect a giant planet with the radius and geometric albedo or effective temperature of Jupiter at 5 AU (scaled by the square root of stellar luminosity) around at least 50% of its target stars. A signal-to-noise ratio of at least 5 is required.

Exozodiacal dust: Emission from exozodiacal dust is both a source of noise and a legitimate target of scientific interest. TPF-I must be able to detect planets in the presence of zodiacal clouds at levels up to a maximum of 10 times the brightness of the zodiacal cloud in the Solar System. Although the average amount of exozodiacal emission in the "habitable zone" is not yet known, we adopt an expected level of zodiacal emission around target stars of 3 times the level in our own Solar System with the same fractional clumpiness as our Solar System's cloud. From a science standpoint, determining and understanding the properties of the zodiacal cloud is essential to understanding the formation, evolution, and habitability of planetary systems. Thus, the mission should be able to determine the spatial and spectral distribution of zodiacal clouds with as little as 0.1 times the brightness of the Solar System's zodiacal cloud.

Spectral range: The required spectral range of the mission for characterization of exoplanets will emphasize the characterization of Earth-like planets and is therefore set to 6.5 to 18 μm in the infrared. The minimum range is 6.5 to 15 μm.

Spectrum: The mission will use the spectrum of a planet to characterize its surface and atmosphere. The spectrum of the present Earth, scaled for semi-major axis and star luminosity, is used as a reference and suggests a minimum spectral resolution of 25 with a goal of 50. The mission must measure water (H_2O) and ozone (O_3) with 20% accuracy in the equivalent width of the spectral feature. Additionally it is highly desirable that the mission be able to measure carbon dioxide (CO_2) as well as methane (CH_4) (if the latter is present in high quantities predicted in some models of pre-biotic, or anoxic planets).

Table 2. Mid-IR Infrared Imaging Mission Requirement Summary

Parameter	Requirement
Star Types	F, G, K, selected, nearby M, and others
Habitable Zone	0.7–1.5 (1.8) AU scaled as $L^{1/2}$ *(Note *)*
Number of Stars to Search	> 150
Completeness for Each Core Star	90%
Minimum Number of Visits per Target	3
Minimum Planet Size	0.5–1.0 Earth Area
Geometric Albedo	Earth's
Spectral Range and Resolution	6–18 μm; R = 25 [50]
Characterization Completeness	Spectra of 50% of Detected or 10 Planets
Giant Planets	Jupiter Flux, 5 AU, 50% of Stars
Maximum Tolerable Exozodiacal Emission	10 times Solar System Zodiacal Cloud

*There are two definitions in the literature for the outer limit of the habitable zone. The first is 1.5 AU scaled to the luminosity to the ½ power based on Kasting et al. (1993). The second is 1.8 AU scaled in the same way from Forget & Pierrehumbert (1997).

Number of stars to be searched: To satisfy its scientific goals, the mission should detect and characterize a statistically significant sample of terrestrial planets orbiting F, G, and K stars. Although at this time, the fractional occurrence of terrestrial exoplanets in the Habitable Zone is not known, a sample of 150 stars within 30 pc (including a small number of nearby M stars) should suffice based on our present understanding.

Extended number of stars: It is desired to search as many stars as possible, beyond the required core sample. We anticipate that any mission capable of satisfying these objectives will also be capable of searching many more stars if the overall requirements on completeness are relaxed. It is desired that the mission be capable of searching an extended group of stars defined as those systems of any type in which all or part of the continuously habitable zone (see below) can be searched.

Search completeness: Search completeness is defined as that fraction of planets in the orbital phase space that could be found within instrumental and mission constraints. We require each of the 150 stars to be searched at the 90% completeness level. For other targets in addition to the 150 stars, the available habitable zone will be searched as to limits in planet's orbital characteristics.

Characterization completeness: While it will be difficult to obtain spectra of the fainter or less well positioned planets, we require that the mission be capable of measuring spectra of at least 50% of the detected planets.

Visitations: Multiple visits per star will be required to achieve required completeness, to distinguish it from background objects, to determine its orbit, and to study a planet along its orbit. The mission must be capable of making at least three visits to each star to meet the completeness and other requirements.

Multiple Planets: After the completion of the required number of visitations defined above, the mission should be able to characterize a planetary system as complex as our own with three terrestrial-sized planets assuming each planet is individually bright enough to be detected.

Orbit Determination: After the completion of the required number of visitations defined above, the mission shall be able to localize the position of a planet orbiting in the habitable zone with an accuracy of 10% of the semi-major axis of the planet's orbit. This accuracy may degrade to 25% in the presence of multiple planets.

In addition to its program of planet detection and characterization, the TPF-I mission would have at least 25% of mission time available for a revolutionary program of general astrophysics, providing a sensitivity to rival JWST but with angular resolution of 1–10 mas, depending on wavelength and array configuration. As described by the TPF-I Science Working group (Lawson et al. 2007), such a facility would make dramatic new observations in areas of: 1) Star and planet formation and early evolution; 2) Stellar and planetary death and cosmic recycling; 3) The formation, evolution, and growth of black holes; and 4) Galaxy formation and evolution over cosmic time.

The highlights of precursor science will include (1) contributions from CoRoT and Kepler to our knowledge of the frequency of terrestrial planets; (2) measurements by the Keck Interferometer and the Large Binocular Telescope Interferometer of exozodiacal emission around nearby stars; (3) spectroscopy of giant transiting exoplanets from HST, Spitzer, and JWST; and (4) contributions from medium-scale strategic exoplanet missions, yet undefined. Spectroscopy of Earth-like planets in extreme or unusual environments (hot Earths, SuperEarths, and Earths around M-dwarfs) may also be forthcoming in the 2010–2020 decade.

2. TECHNICAL OVERVIEW

In the mid-infrared the required angular resolution of ≤50 mas would necessitate a single telescope with a primary mirror larger than 40 m across, making an interferometer a compelling choice for the overall design. Nulling interferometry is used to suppress the on-axis light from the parent star, whose photon noise would otherwise overwhelm the light from the planet. Off-axis light is modulated by the spatial response of the interferometer: as the array is rotated, a planet produces a characteristic signal which can be deconvolved from the resultant time series (Bracewell 1978; Woolf and Angel 1998). Images of the planetary system are formed using an extension of techniques developed for radio interferometry (Lay 2005).

Mission Architecture and Trade Studies

Several interferometer implementations have been studied in the past decade. A structurally-connected version with a deployable 36-m boom was studied (the maximum size that can be accommodated in the launch shroud), but the 90 mas inner working angle and poor angular resolution greatly restricted its capability for finding Earth-like planets. Tethered spacecraft were also considered and rejected. Formation-flying has become the platform of choice for both NASA and ESA, and after many years of study, the architecture for TPF-I that seems the most promising is the *X-Array*, configured in an out-of-plane geometry known as the *Emma* design.

The X-Array: An architecture trade study in 2004 favored the X-Array over other architectures (Lay et al. 2005). The X-Array is configured as two pairs of telescopes, where each pair acts as a separate nulling interferometer. The distance between telescopes in each pair therefore can be tuned to best suppress background stellar leakage around the null. Then the distance between one pair and the other can be adjusted to provide the angular resolution necessary to unambiguously isolate the light from a planet. In most other designs, the baselines for nulling are coupled with those that provide the angular resolution — and in those designs it is difficult to simultaneously suppress stellar leakage *and* have high angular resolution. The X-Array has other advantages: it uses only two types of spacecraft designs, has a simple beam-relay geometry, and its performance degrades gracefully, should a reflector spacecraft be lost. The X-Array also provides a means of eliminating noise due to "instabilities" in the servo systems that maintain the null. Instability in the null — the analog of speckle noise in a coronagraph — can otherwise mimic the fringe modulation due to the presence of a planet. With the X-Array design, a null depth to 10^{-5} would satisfy the flight requirements (Lay 2006).

Emma Design: ESA, as part of its design studies, considered the "Emma" architecture, shown in Figure 2. In this design the combiner is moved out towards the star by about 1 km, and the collectors are reduced to simple spherical mirrors. The Emma design offers significant advantages which have been studied independently by ESA and NASA. The appeal of the Emma design is primarily in its simplification of the collector spacecraft: a complete optical system is eliminated and the layered sunshields are now protected by a hard shell. The collector diameter can be scaled up or down to suit the mission performance requirements, with minimal impact on the combiner design.

Mission Design

The baseline design for the mission is summarized in Table 1. The observatory comprises 5 spacecraft, being four identical 2-m meter collectors and one combiner spacecraft, but with an additional cruise stage to bring the observatory to its Sun-Earth L2 halo orbit. TPF-I is a Large-class mission; the numbers that are presented in this section stem from a Team-X Study at JPL conducted in early 2009 based on the Emma X-Array. This was the only occasion that Team-X

had studied this design, and future improvements in the design (notably a reduction in total mass) are to be expected.

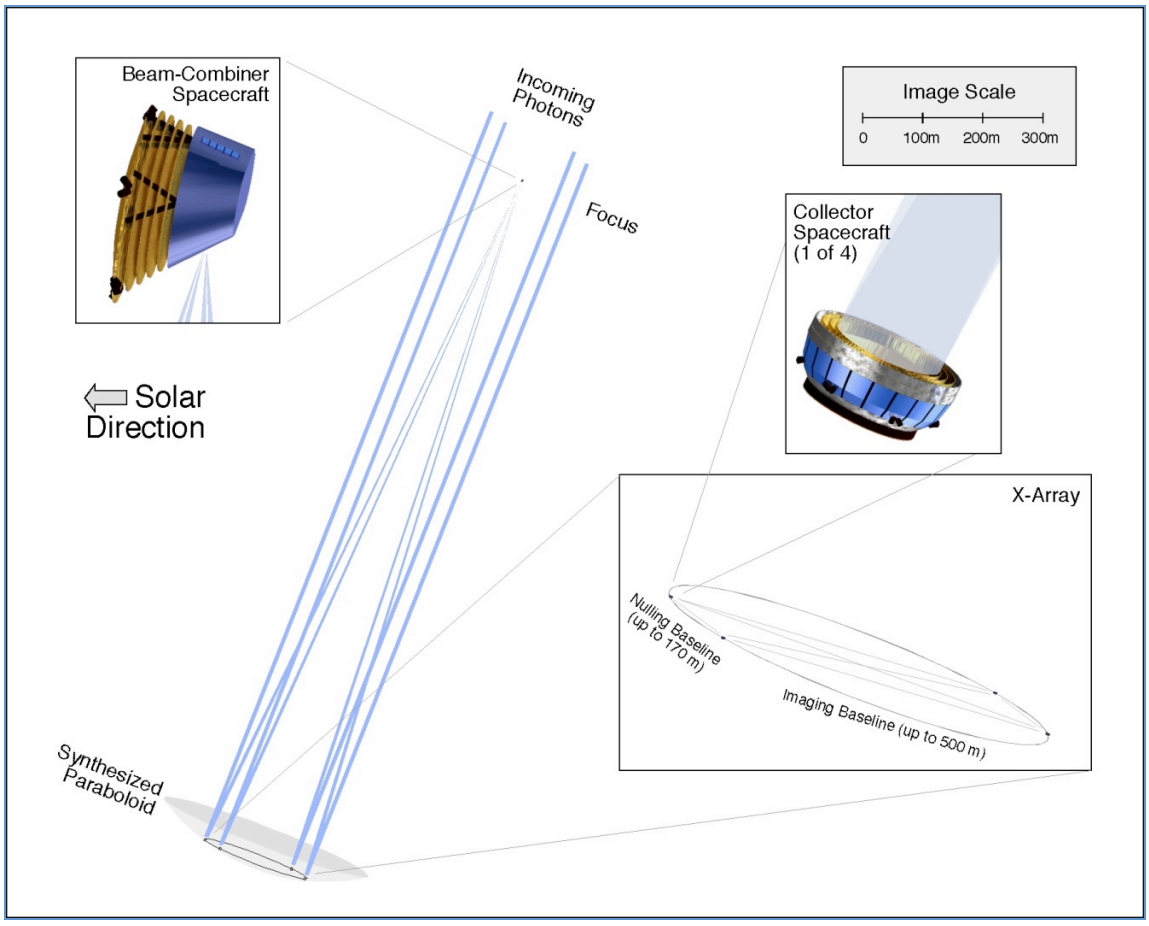

Figure 2. The architecture of the Emma X-Array. The four collector spacecraft, each with a 2-m mirror, are distributed in a rectangular array about 1200 m from the beam-combining spacecraft. The array is pointed between 45º and 90º to the anti-Sun direction, thus providing almost full-sky coverage during the course of a year. [Courtesy of T. Herbst (MPIA) and Thales Alenia Space]

Launch: The total mass-to-orbit is high, 8200 kg, and would require a large-class launch vehicle, such as the Delta IV H-19. This mass estimate includes the combiner (1770 kg), four identical collectors (1190 kg each), and a cruise stage (1670 kg). All six spacecraft are launched together: the collectors are stacked one top of each other on the combiner, which in turn sits atop the cruise stage that brings the observatory to its L2 halo orbit.

Power Requirements: The maximum power mode on the combiner is 4570 Watts. The maximum power mode on each collector is 720 Watts and is accommodated with fixed solar arrays built around the collector's thermal shade. The maximum power needed in the cruise stage is 550 Watts.

Observing scenario: The combiner spacecraft is responsible for orienting the four collector spacecraft, each collector being exact duplicates. A direct to Earth S-band telecom system will be available on each collector in case of an anomaly, but normal operations would be coordinated through the combiner, via another S-band link on a different channel. In science-mode observations, the four collector spacecraft are distributed in a rectangular configuration

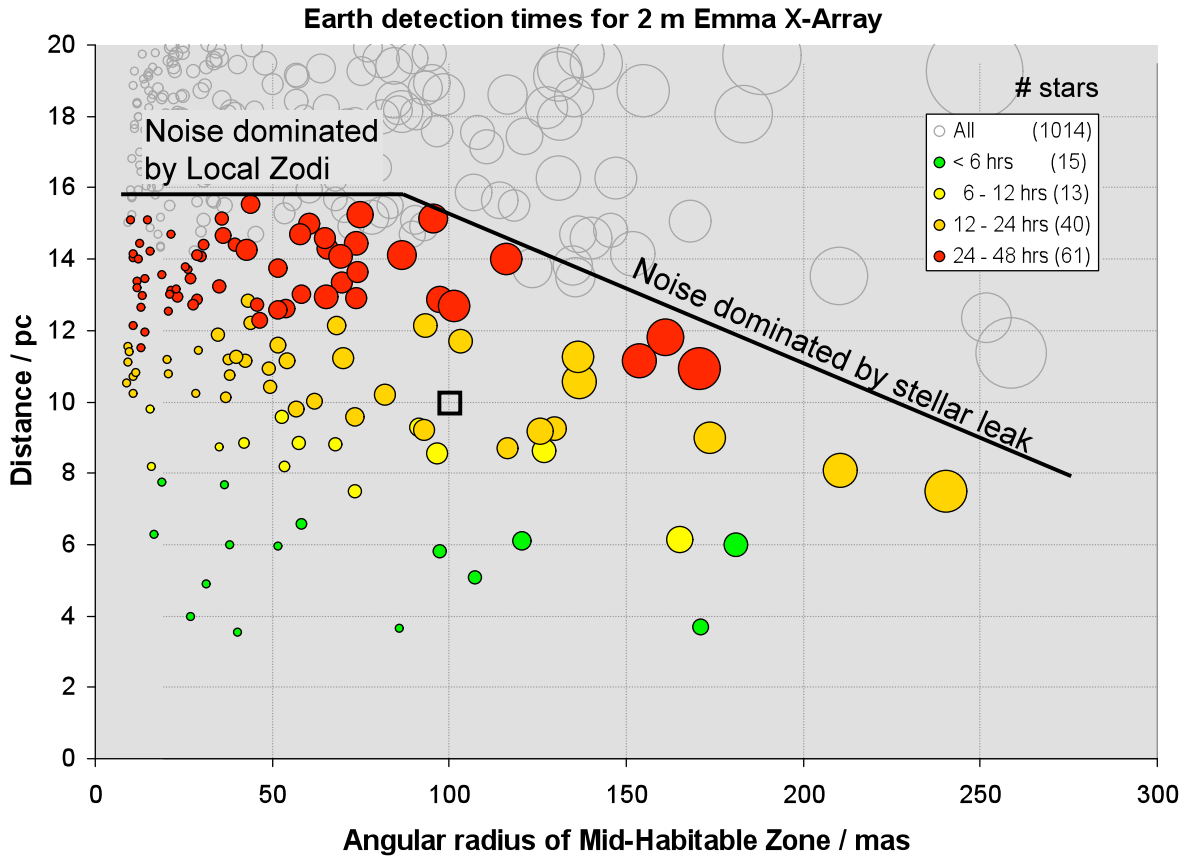

Figure 3. The integration time required per target for a signal-to-noise ratio of 5 for an Earth-sized planet at the center of the habitable zone.

whose edge distances have a 1:6 ratio. The separations on the short side of the rectangle provide the nulling baselines that provide starlight suppression. The separations on the longer sides provide the imaging baselines that provide the angular resolution needed to detect Earths and to separately distinguish multiple planets. The combiner is located 1200 m away, and the whole forms a dilute aperture which is pointed between 45º and 90º to the anti-Sun direction. During an observation, the orientation of the combiner remains fixed, while the array of collector spacecraft is rotated about the array's center. Steering mirrors at the entrance of the combiner, one for each collector, track the circular paths of the collectors during a rotation. The collectors will have separations between 20 and 400 m, and require the control of their relative positions not to nanometers, but to within several tens of centimeters. This relaxed control of the collectors is possible because the combiner uses four delay lines, driven by fringe tracking, to provide the long path adjustment and the nanometer-level control necessary to phase the starlight.

Performance Model

Performance Model: The Interferometer Performance Model breaks down the contributions to the SNR for a single observation, including both photon noise and instability noise. Figure 3 shows the integration times required to achieve an SNR of 5 for an Earth-sized planet at the center of the habitable zone, for each of 1014 candidate target stars. Circle diameters are

proportional to the intrinsic size of the star. Large circles to the upper right are F stars; small circles to the lower left are late K or early M spectral types. The array properties are listed in Table 1. In contrast to a fixed structure or primary mirror, formation-flying interferometry allows a flexible array size that can be tailored to maximize the SNR for each star. The long baselines are sufficient to resolve the habitable zone around all nearby stars. Planets are easiest to detect around nearby K stars. Integration times increase through the A and F stars as a result of the higher stellar leakage. For the Earth-Sun system at 10 pc (square symbol), 14 hours of integration time is required for detection. The Interferometer Performance Model is the source of requirements on both the flight system and the technology testbeds, and provides inputs to the mission-level model.

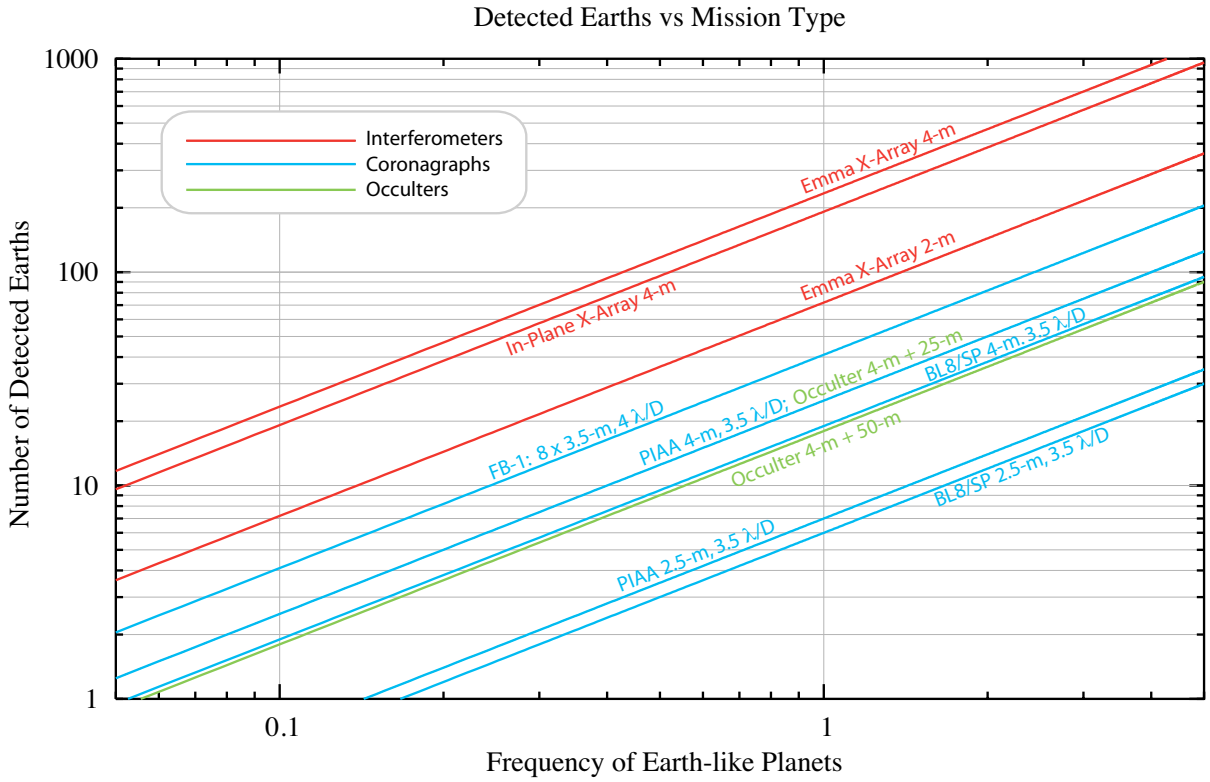

Figure 4. Comparison of the predicted performance of interferometer (Emma X-Array), coronagraph, and occulter architectures, scaled from predictions assuming there is one Earth-like planet around every target star (Frequency of Earth-like Planets = 1). Architectures with different primary mirror sizes are illustrated.[1]

The mission-level model estimates the number of target stars observable in a given mission duration. The algorithm optimizes the observing schedule to maximize the number of planets found in the habitable zone. Based on the same completeness analysis developed for TPF-C, the model uses a Monte Carlo distribution of planetary orbits, includes a high-fidelity representation of the instrument, and accounts for which targets are available during each week of the mission. We assume that 2 years of the nominal 5 year mission are set aside for the initial survey, including overheads for re-targeting, calibration, etc. Each target requires only a single visit in the optimized scenario, resulting from the combination of the very small inner working angle and, in the mid-infrared, a constant planet-brightness throughout each orbit. If every star has one Earth-sized planet, randomly distributed over the range of possible habitable orbits, then an Emma X-Array with 2-m collectors can detect an average of 72 Earths by observing 153 target

stars. Observations of nearby stars have a completeness close to one, i.e. almost all potentially habitable planets are detected, but as the distance increases it proves to be most productive to observe a larger number of stars at lower completeness than fewer stars at high completeness. In this case the net completeness for the survey is ~47%. For 4-m collectors the average planet yield increases to 230 with 450 targets. Figure 4 shows how these values compare with various coronagraph and occultor designs, that use the very same optimization. The lines represent the points for one Earth per star, scaled linearly to other values. The data is drawn from the Navigator whitepaper submitted to the Exoplanet Task Force.[1,2]

Candidate detections require 2–3 follow-up observations to establish the orbit and discriminate against background sources. Again, TPF-I's angular resolution and compact inner working angle are ideally suited to the task. The resolution of a stretched X-Array (210 × 35 m) is illustrated in the dirty map shown in Figure 5, synthesized from multi-channel observations. Planet locations are marked with an '×'; the negative mirror images are a side-effect of phase chopping, and are eliminated in the deconvolution process.

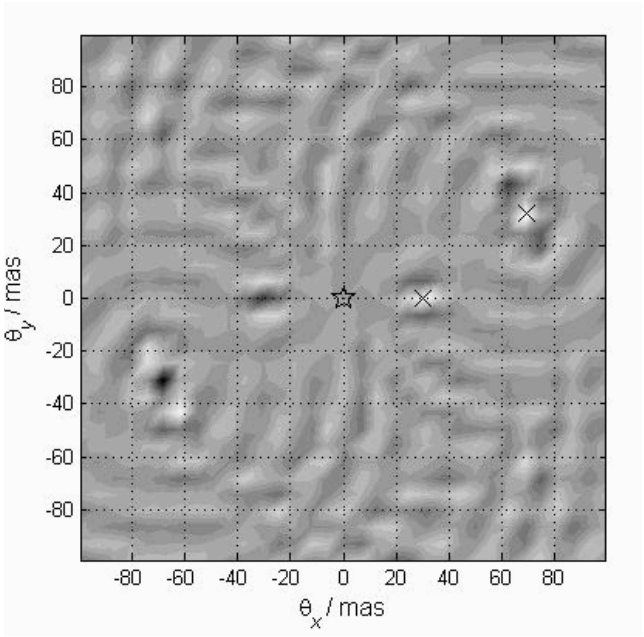

Figure 5. Resolution of a stretched X-Array (210 x 35 m). The target star is in the center of the field with planet locations shown by the crosses.

Simultaneous full resolution (R~100) spectroscopy for all objects within the field of view is a natural by-product of interferometric observing. While data from the detection and orbit determination phases should be sufficient for a coarse spectrum, a deep characterization will require significant integration time. Detection of CO_2 for an Earth at 5 pc with 2-m collectors will require ~24 hours of integration (SNR of 10 relative to the continuum). The narrower ozone absorption line requires 16 days at 5 pc. For ozone at 10 pc, integration times as long as 40 days could be needed, falling to ~6 days with 4-m diameter collectors. Integrating deep into the noise for these observations is made possible by the very specific combination of modulations imprinted on the planet signal that distinguish it from the noise: a characteristic low frequency variation from array rotation, the fast switching of phase chopping, and the oscillating wavelength dependence of the interferometric response in the spectral domain.

[1] http://exoplanets.jpl.nasa.gov/documents/NP_sci_overview_070402_final-traub.pdf

[2] In the figure "FB-1" is the TPF-C Flight Baseline design with a 3.5 × 8 m primary and inner working angle of 4 λ/D; "BL8" is a band-limited 8th order mask coronagraph; "SP" is a shaped pupil mask coronagraph; "PIAA" is a Phase-Induced Amplitude Apodization coronagraph; the occultors shown have a 50-m shade at 72,000 km and a 20-day slew, and a 25-m shade at 30,000 km and a 6-day slew (in each case a telescope with a 4-m primary is assumed). The inner working angle in all cases is 3.5 λ/D, except for FB-1 which uses 4 λ/D. In all the examples, the yield scales linearly with the prevalence of Earth-like planets.

3. TECHNOLOGY DRIVERS

The technology tall poles for TPF-I are 1) Formation flying technology; 2) Nulling interferometry; and 3) Cryogenic engineering.

Formation Flying

The principal objective of formation flying is to control the relative locations of separated spacecraft so that the beams of starlight that are sampled by each telescope travel the same distance from the star to the beam combiner. At the combiner spacecraft, each optical beam will have its own delay line with sub-nanometer resolution, with up to a meter of adjustable delay prior to beam combination. In this way, the separated spacecraft need only be controlled in their relative positions at the level of several tens of centimeters.

The formation-flying array will be launched into orbit far from the Earth, and on-board autonomy will be essential. Multiple spacecraft in a formation necessitate a distributed architecture for relative sensing, communications, and control; each spacecraft in the formation must sense the relative location of its neighbors and relay this information to each of the other spacecrafts. A hierachical and distributed control algorithm is needed to guide the maneuvers. The maneuvers must also be orchestrated to conserve and balance the consumption of propellant amongst the elements of the array. The overall formation architecture needs to support a high degree of system robustness. Specialized abilities, such as formation acquisition and collision avoidance, must be designed into the control algorithms to make the system fault-tolerant and to avoid catastrophic mission failure.

There has been much interest in formation flying technology, both in Europe and the United States. Ground-based simulations and testing[3], have validated the control algorithms that are required for science observations with a formation-flying interferometer. TPF-I will require formation flying technology to control the relative positions of satellites that are several tens of meters to several hundred meters apart with a resolution of several centimeters to several tens of centimeters. So far in-space testing has tested 1) rendezvous and docking exercises in close proximity; and 2) the relatively loose control of constellations of spacecraft with many kilometers of separation. In Earth-orbit, where these experiments have been undertaken, GPS sensing can be used to obtain absolute position information at the level of a few centimeters. (No such positioning system will be available in the Sun-Earth L2 orbit that TPF-I will use.) Examples of this work include the Orbital Express mission, which demonstrated in 2007 the separation, docking and transfer of materials from one spacecraft to another. Also ESA's Jules Verne Automated Transfer Vehicle demonstrated in 2008 docking with the International Space Station. The only precision formation flying technology to be tested in space so far are the control algorithms of the SPHERES testbed of MIT, flown within the International Space Station.

The guidance, navigation and control algorithms that have been demonstrated on the ground now need to be proven in space. The interferometric combination of light from separated telescopes in space also needs to be demonstrated. Some of this work is already underway: the Swedish Prisma mission will test Darwin (TPF-I) RF metrology using microsatellites to be launched in June 2009; ESA's Proba-3 mission will test RF and optical metrology and use cold-gas and electrical micro-propulsion for actuation. However, a longer campaign and a follow-on

[3] "TPF-I Technology Milestone #2 Report: Formation Control Performance Demonstration," edited by D. P. Scharf and P. R. Lawson, JPL Pub. 08-11: http://planetquest.jpl.nasa.gov/TPF-I/TPFI_M2_ReportV3.pdf

mission of in-space validation of interferometry using separated platforms needs to be supported by NASA to enable a flagship mission such as TPF-I. This would be possible through international collaboration with a US contribution in the range of $160M.

Mid-IR Nulling Interferometry

In an ideal nulling interferometer, the electric fields of the light from the collecting telescopes are combined with a prescribed set of amplitudes and phases that produce a perfect null response in the direction of the star. In practice, vibrations and thermal drifts result in small path-length errors and time variable aberrations; the null floor is degraded and there is a time-variable leakage of stellar photons that can mimic a planet signal. This has become known as instability noise. Our analysis shows that a null depth of 10^{-5} is generally sufficient to control the level of photon noise arising from the stellar leakage (arising from the interferometer beginning to resolve the star), but that a null of 10^{-6} is needed to prevent instability noise from becoming the dominant noise source. A null of 10^{-6} requires an RMS path control of ~1.5 nm, and an RMS amplitude control of ~ 0.1%. Under these circumstances, instability noise, rather than photon noise, drives the performance of the instrument.

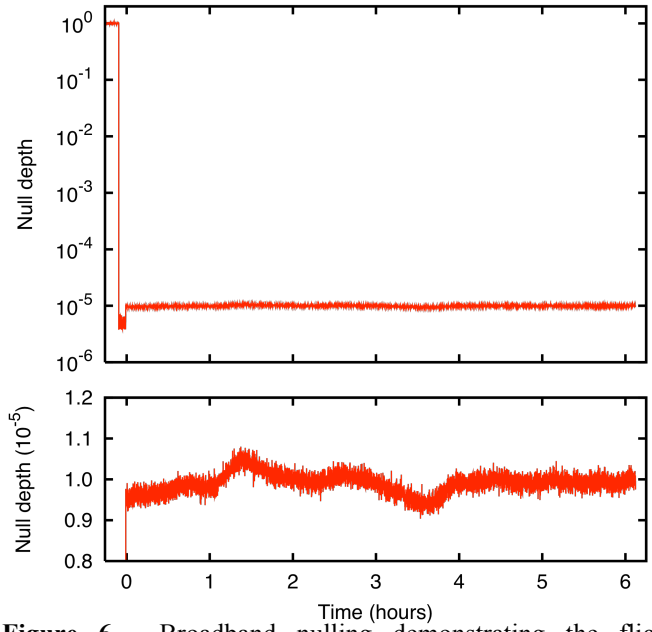

Figure 6. Broadband nulling demonstrating the flight requirement of 1 x 10^{-5} over a 6-hour experiment. A central wavelength of 10 microns and a bandwidth of 34% was used. The top shows the full trace, including reference and noise measurements, followed by nulling data which begin at time "0." The bottom trace shows the nulling data on a linear scale.

Lay (2006) proposed to spectrally filter the data to effectively remove the signature of instability noise. With spectral filtering it becomes possible to relax the required null depth by a factor of 10 or more, to 10^{-5}. In the absence of instability noise, the SNR is determined by photon noise, with principal contributions from stellar size leakage, local zodical dust, and stellar-null floor leakage. Relaxing the null depth to 10^{-5} has only a small impact on the SNR.

By late 2008, laboratory demonstrations[4,5] had succeeded in surpassing the revised flight requirement of a null depth of 1×10^{-5}, as illustrated in Fig. 6. Experiments with the Adaptive Nuller testbed met this goal using unpolarized light with a bandwidth of 34%, centered at $\lambda = 10$ μm (Peters et al. 2008, 2009), and related work validated the overall approach used for achromatic phase shifting (Gappinger et al. 2009).

[4] "TPF-I Technology Milestone #1 Report: Amplitude and Phase Control Demonstration," edited by R. D. Peters, P. R. Lawson, and O. P. Lay, 2007, http://planetquest.jpl.nasa.gov/TPF-I/TPF-I_M1Report_Final_signatures.pdf

[5] "TPF-I Technology Milestone #3 Report: Broadband Starlight Suppression Demonstration," edited by R. D. Peters, R. O. Gappinger, et al., 2009, JPL Document D-60326: http://planetquest.jpl.nasa.gov/TPF-I/TPF-I_M3_Report_023_small.pdf

An Earth-like planet would, however, be ~10^{-7} fainter than a Sun-like star, and so an additional noise suppression of a factor of 100 is yet needed to suppress the local and exozodiacal background that would be typically observed. Room temperature experiments are underway with the Planet Detection Testbed at JPL to demonstrate this additional suppression, as well as providing a proof-of-concept for instability noise suppression by spectral filtering.

The remaining tall poles for nulling development are the engineering demonstrations of cryogenic breadboard and brassboard instrument designs. This would include preliminary tests of components, such as fibers and deformable mirrors, followed by subsystem testing of delay lines and adaptive nullers, and ultimately a cryogenic four-beam testbed similar to the Planet Detection Testbed. This work would include full coverage of the 6–18 micron science band, as well as the simulated detection of biomarkers. Support at the level of $140M in the 2010–2020 decade would allow the development this technology so that it is ready for flight implementation.

Cryogenic Optics and Engineering

At mid-infrared wavelengths every warm object emits radiation, and warm surfaces within the observatory, such as the telescope and interferometer optics, can appear far brighter than the astronomical sources that might be observed. The optics must therefore be cooled, shielded from direct sunlight, and provided with baffling and protection against scattered light. Using a multi-layered thermal shield, passive cooling to 50 K seems feasible with technology developed for JWST and should be adequate for TPF-I. Although adequate thermal shielding will be crucial to the success of the mission, the project has not considered this to be a technology tall pole.

Unlike most cryogenic observatories, that are designed to have very few moving parts and actuators, the TPF Interferometer will have numerous active systems within the combiner. These will likely include movable mirrors for alignment and star acquisition, multi-stage delay lines for pathlength control, piezoelectric actuators for pathlength modulation, and shutters for alignment and calibration. Each of these devices will dissipate heat and induce vibrations in the structure. Many of the strategies that are currently used to limit vibrations in room-temperature interferometers will be adapted and used at cryogenic temperatures. Each device will need to meet a global heat-dissipation error budget if the interferometer is to remain within operational temperature limits. As well, the structural behavior and damping properties of the observatory will change at extremely low temperatures, offering a challenge for a system that is particularly susceptible to vibration. Therefore, with regard to cryogenic engineering, the tall pole is cryogenic system engineering for an inherently complex system.

TPF-I will need state-of-the-art coolers for its detectors. Over the last two decades, NASA, often in collaboration with the US Air Force, has funded cryocooler technology development in support of a number of missions. The largest use of coolers is currently in Earth Science instruments operating at medium to high cryogenic temperatures (50 K to 80 K), reflecting the current state-of-the-art cryocooler technology. Since 2002, two new long-life cryocooler systems have been launched into space to support NASA missions: the Northrop Grumman Space Technology (NGST) pulse tube coolers on the Atmospheric Infrared Sounder (AIRS) instrument, and the Creare NCS turbo Brayton cooler (on the Hubble Space Telescope's Near Infrared Camera and Multi-Object Spectrometer, NICMOS, instrument.) Up until 2005, NASA sponsored the development of cryocooler technology to be shared between TPF, Con-X, and JWST. In 2005 that effort was taken over entirely by JWST. By then it had met the TPF pre-Phase A goal of demonstrating 20 mW of cooling at 6 K, and 150 mW at 18 K with about 250 W of input power with a Lockheed-Martin four-stage pulse tube cryocooler. This work would need to be revisited and adapted to TPF-I, with a particular attention to vibration requirements.

4. ORGANIZATION, PARTNERSHIPS, AND CURRENT STATUS

NASA provided directed funding to develop TPF technology beginning early in the 2000–2010 decade. In 2003 NASA entered into a Letter of Agreement with the European Space Agency (ESA) to select by 2006 a common interferometer mission architecture with the Darwin mission. NASA's objective was to choose the best architecture for TPF based on scientific and technological readiness of the various candidate designs.

The TPF Science Working Group (TPF SWG), and subsequently the TPF-I SWG, refined the science requirements, as listed in Section 1, in collaboration with ESA's Terrestrial Exoplanet Science Advisory Team (TE-SAT). Parallel work in Europe and the US developed models and tools to predict the mission performance, as well as parallel catalogs of target stars.

Future technology efforts would be coordinated by NASA through the Exoplanet Exploration Program and leverage the already successful work of the testbeds at the Jet Propulsion Laboratory. Anticipated partners for the proposed program would include national and international agencies in Europe, under arrangements yet to be discussed and negotiated.

Current Status

Technology development for TPF-I has been extremely successful. Highlights of technology development have included the following:

1. Broadband nulling has been demonstrated to the null depth required in flight, over a 34% bandwidth centered on 10 microns. (Peters et al. 2008, 2009)
2. Single-mode mid-IR fibers have been demonstrated at 10-microns using both chalcogenide glass and silver halide materials, providing the required spatial filtering performance. (Ksendzov et al. 2007, 2008)
3. Cryogenic delay lines have been demonstrated by the European Space Agency.
4. Formation flying algorithms have been demonstrated in the laboratory, using a robotic testbed, to have the performance required for flight (Scharf et al. 2008).
5. The architecture trades studies in the US and Europe converged in 2007, leading to the Emma X-Array, described previously.
6. Target catalogs and observatory performance models developed independently in Europe and the US were shown to be in close agreement.
7. Experiments within the International Space Station (using MIT SPHERES), as well as in space with rendezvous and docking (Orbital Express and ESA's ATV Jules Verne) have demonstrated GPS and video-based control of separated satellites.
8. Precursor formation flying missions are now in formulation (ESA's Proba-3) and in preparation for launch (Swedish Space Corporation's Prisma) to test RF metrology, optical metrology, and cold-gas and electrical micro-propulsion.

Although NASA has indefinitely deferred plans for a TPF mission, it has continued to fund research in interferometer (and coronagraph) technology with the goal of enabling a mission of reduced scope from the missions that had been envisaged earlier in the decade.

The angular resolution required of a mid-infrared mission dictates a physical size for the observatory of 40 m or more if spectra of Earth-like planets are to be measured. For this reason alone, a mid-infrared mission, as described in these pages, continues to be a flagship-class mission based on formation-flying technology.

Researchers at JPL continued to collaborate with the Darwin mission PI, Prof. Alain Léger, and are now completing the room-temperature demonstrations with the nulling testbeds, which in 2009–2010 will focus on four-beam system-level planet detection experiments in the lab.

5. TECHNOLOGY & MISSION DEVELOPMENT SCHEDULE

The proposed technology development, as outlined in Table 3, will complete the vacuum cryogenic nulling technology and engineering, and demonstrate separated-platform interferometry in space.

The initial technology effort would be focused on the verification and validation of mid-infrared nulling interferometry in a flight-like environment. All experiments in nulling interferometry for TPF-I have been conducted at room-temperature at wavelengths near 10 microns. The proposed activities would extend these experiments to a flight-like environment (temperatures approaching 50 K and in vacuum) and validate the instrument models and error budgets to arrive at a high-fidelity optical, thermal, and mechanical model of the observatory.

Table 3. Technology Development Schedule

Activity	Timeline	Cryogenic Nulling Interferometry
Component validation	Years 1–2	Cryogenic testing of components, including single-mode mir-IR fibers, fast steering mirrors, actuators, and deformable mirrors
Subsystem validation	Years 3–5	Cryogenic testing of subsystems, including delay lines, achromatic phase shifters, and an adaptive nuller
System testing	Years 6–9	Cryogenic system testing of 4-beam nulling interferometry in a flight-like environment with flight-like hardware: planet signal extraction using array rotation and chopping; instability noise suppression; biomarker characterization
Activity	**Timeline**	**Formation Flying**
Space-based Formation Flying Demonstrations	Years 1–9	Collaboration in space-based experiments in guidance, navigation & control, including thruster and sensor technology, and interferometric beam combining

Research on formation flying in the first half of the 2010–2020 decade has already been defined through anticipated programs at DARPA and by ESA and European national space agencies. However, missions beyond Proba-3 have not been defined. We therefore propose that early in the decade, work on formation flying should be renewed through NASA participation in formation flying experiments with European collaborators, with a launch near 2017. By 2015, initial experiments to verify and validate the performance of thrusters and sensors should have been largely completed. The proposed work is to participate in experiments in multi-platform interferometric beam combination.

A sample schedule for the TPF-I mission to follow is given in Figure 7. This schedule was provided by Team-X as appropriate for a mission of TPF-I's complexity. The start date in this illustration is indicated as 2012; the actual start would follow the completion of the technology program as proposed above. For the mission, Phase A and Phase B are 15 months each. Phase C is 39 months, with 24 months allocated to design, and 15 months to fabrication. Phase D is 22 months, with 16 months allocated to system integration and test, 3 months to pre-launch operations, 2 months transit to Earth-Sun L2, and 1 month to formation stabilization and mirror cool down. Phase E is 61 months, with 1 month allocated to science instrument check-out and calibration; and 60 months of scientific data collection.

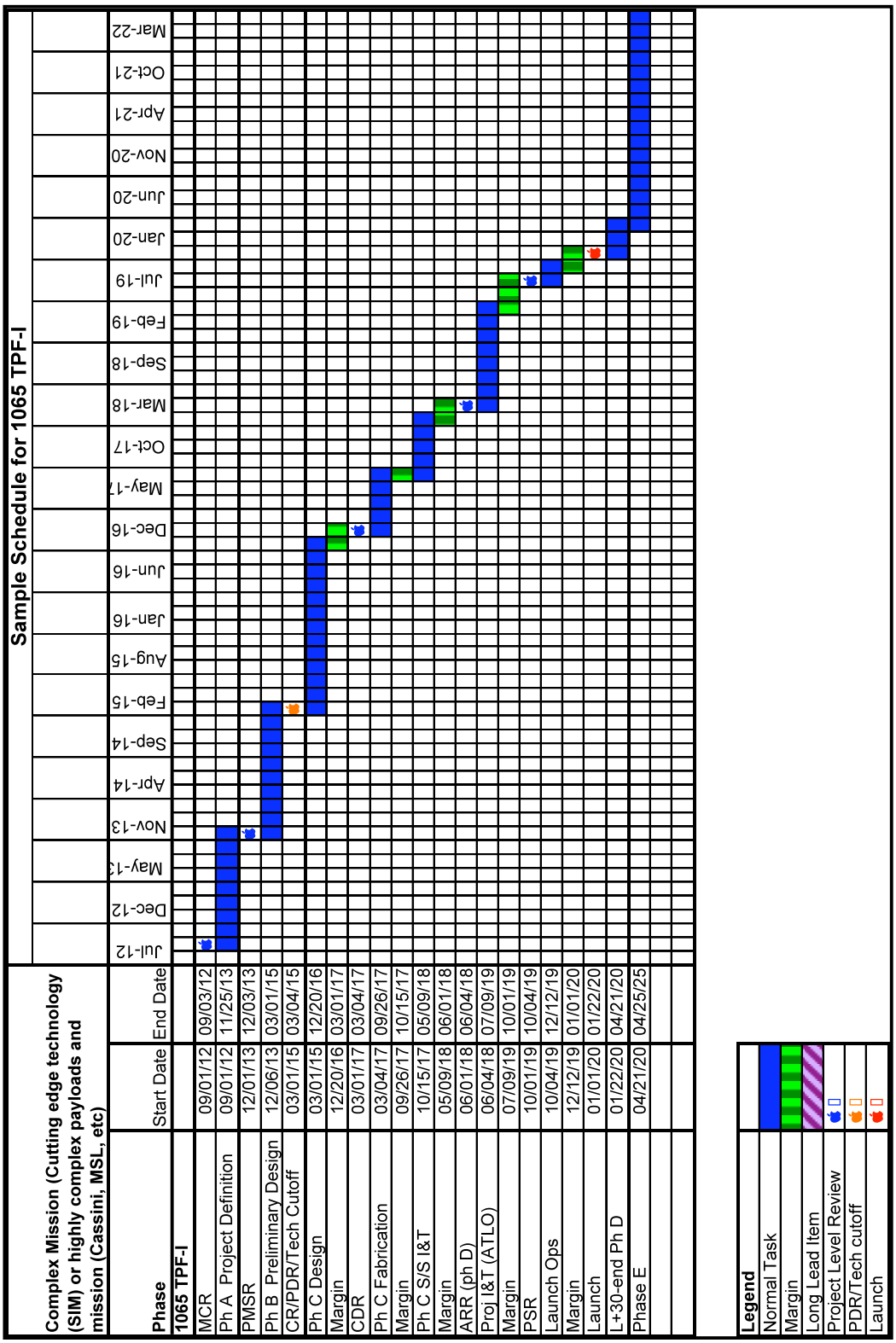

Figure 7. Schedule for TPF-I mission development based on a model used for highly complex payloads or those employing advanced or cutting edge technology. The actual start date would begin at the completion of the technology program described previously, and not 2012 as indicated in this sample schedule.

6. COST ESTIMATES

Technology Development

An investment at the level of $300M in the 2010–2020 decade would advance nulling interferometry and formation flying activities to a level of maturity that would enable TPF-I. An estimated $160M for the decade would provide support for the advancement of nulling interferometry to TRL 6. An additional estimated $140M would fund the US contribution to an international collaboration in formation flying, including space-based experiments in multi-platform guidance, navigation and control, thruster and sensor technology, and interferometric beam combination. This would build on planned US and European experiments in space and bring formation flying technology to TRL 9.

Mission Costs

Cost estimates for the mission were generated as part of a Pre-Phase-A preliminary concept study conducted by Team-X at JPL in January/February 2009. These costs are not included here, because the cost of the payload (combiner and reflectors) was deemed to have a high amount of uncertainty. The instrument is large and complex and beyond the range of the Team-X models. Because the cost of the instrument was estimated to be more than half of the total mission cost, the total costs were not considered by Team-X to be well estimated. Team-X recommended that a grass-roots cost estimate be done for the instrument and the total project cost be re-examined.

The Emma X-Array architecture provides a significant simplification and reduction in cost compared with previous TPF-I designs. Given its innovative nature, it is yet difficult to accurately estimate its cost, though it is certainly in the “flagship” class. Future work will explore additional simplifications to the design, detail a more accurate instrument cost, and in so doing refine the overall cost estimate.

No formal plans exist for cost sharing with other agencies. TPF-I provides an ideal opportunity for international partnership.

7. CONCLUSION

TPF-I has unrivalled angular resolution, vital for unambiguous orbit determination, robust separation of multiple planets, and discrimination against structure in the exozodiacal disk. In these regards, TPF-I far exceeds the predicted capability of other planet-finding missions. Over and above its planet-finding capability, the 2000 Decadal Survey noted "there will be few areas of astrophysics untouched by the power of an infrared interferometer with the resolution and sensitivity of TPF."

This research was carried out through the Jet Propulsion Laboratory, California Institute of Technology, under contract with the National Aeronautics and Space Administration.

8. REFERENCES

TPF-I Website: http://planetquest.jpl.nasa.gov/TPF-I/tpf-I_index.cfm

Beichman et al. 1999,The Terrestrial Planet Finder, JPL Pub. 99-3

Bracewell, R. N. 1978, Nature, 274, 780

Cockell, C. S. et al. 2009, Astrobiology, 9, 1

DesMarais, D. J. et al. 2002, Astrobiology, 2, 153

Forget, F., & Pierrehumbert, R. T. 1997, Science, 278 1273

Gappinger, R. O. et al. 2009, Appl. Opt. 48, 868

Kaltenegger, L., et al. 2007, ApJ, 658, 598

Kasting, J. F. 1993, Icarus, 101, 108

Kasting, J. F. 2005, Precambrian Res., 137, 119

Ksendzov, A. et al. 2007, Appl. Opt. 46, 7957

Ksendzov, A. et al. 2008, Appl. Opt. 47, 5728

Lawson, P. R. & Dooley, J. A., 2005, JPL Pub. 05-5

Lawson, P. R., & Traub, W. A. eds., 2006, JPL Pub. 06-5

Lawson, P. R., et al. eds., 2007, JPL Pub. 07-1

Lawson, P. R., et al. eds., 2009, JPL Pub. 09-3.

Lay, O. P., et al. 2005, Proc. SPIE, 5905, 8

Lay, O. P. 2004, Appl. Opt. 43, 6100

Lay, O. P. 2005, Appl. Opt. 44, 5859

Lay, O. P. 2006, Proc. SPIE, 6268, 62681A

Lovelock, J. E. 1975, Proc. R. Soc. London B, 189, 167

Lovelock, J. E. 1980, Cosmic Search, 2, (4), 2

Martin, S. R., et al. 2003, Proc. SPIE, 5170, 144

Martin, S. R., et al., JPL Doc. D-47627

Peters, R. D., et al. 2008, Appl. Opt. 47, 3920

Peters et al. 2009, PASP, in preparation

Sagan, C., et al. 1993, Nature, 365, 715

Scharf, D. P, et al. 2008, JPL Pub. 8-11

Segura, A., et al. 2003, Astrobiology, 3, 689

Selsis, F., et al. 2002, A&A, 388, 985

Wallner, O., et al. 2007, Proc. SPIE, 6693, 66930U

Woolf, N., & Angel, J. R.1998, Ann. Rev. Astron. Astrop., 36, 507